Archive of Applied Mechanics 63 (1993) 534–542

Archive of
Applied Mechanics

Analytical buckling solutions for circular Mindlin plates: inclusion of inplane prebuckling deformation

G. M. Hong, C. M. Wang and **T. J. Tan,** Singapore

Summary: The buckling problem of thick circular plates under uniform radial loads with allowance for inplane prebuckling deformation is solved analytically. The analytical buckling solutions should be very useful as benchmark values for testing the validity, convergence and accuracy of numerical techniques for plate buckling. This study shows the importance of including the prebuckling deformation in thick plate buckling since its effect is in the same order of magnitude as that of shear. The prebuckling deformation effect raises the critical load and is more pronounced in clamped plates than in simply supported ones as the former plates undergo greater deformation before buckling.

Analytische Lösungen für das Ausbeulen von Mindlin-Platten: Berücksichtigung der ebenen Vorbeul-Verformung

Übersicht: Es wird das Ausbeulproblem von dicken, kreisförmigen Platten, die gleichförmigen radialen Lasten ausgesetzt sind, unter Berücksichtigung der ebenen Vorbeul-Verformung analytisch gelöst. Die analytischen Beullösungen sollten als Anhaltswerte für Untersuchungen der Gültigkeit, Konvergenz und Genauigkeit von numerischen Verfahren sehr nützlich sein. Die Untersuchung zeigt auch, daß es wichtig ist, die ebene Vorbeul-Verformung beim Ausbeulen dicker Platten zu berücksichtigen, weil dieser Einfluß von derselben Größenordnung ist wie der der Scherung. Der Effekt der Vorbeul-Verformung erhöht die kritische Last und ist bei fest eingespannten Platten stärker ausgeprägt als bei einfach gelagerten, weil erstere vor dem Verbeulen größere Deformationen erfahren.

1 Introduction

It is well-known that shear deformation (*SD*) influences the critical loads of moderately thick plates. The neglect of this *SD* leads to an overprediction of the critical load, with increasing error as the thickness-length ratio increases. The *SD* effect can be incorporated using the first order shear deformation (Reissner-Mindlin) theory [1, 2]. The governing equations for Mindlin plate buckling were first derived by Kollbrunner and Herrmann [3] and a more general version of the equations which include vibratory effects was given by Herrmann and Armenakas [4]. A study by Srinivas and Rao [5] has shown that this first order theory will suffice in giving reasonably accurate buckling solutions after comparing with results derived from a three-dimensional exact analysis. In 1983, Ziegler published an interesting paper [6] where he showed that the effect of inplane prebuckling deformation (*PBD*) is of the same order of magnitude as the shear effect on a simply supported rectangular plate. Recently, Xiang et al. [7] further investigated the effect of *PBD* on thick rectangular plates with various edge conditions, thickness-length ratios, aspect ratios and Poisson's ratios. It was found that the *PBD* is even more significant when the plates:

(a) are subjected to a combination of compression loadings in one direction and tensile loadings in the other orthogonal direction,
(b) have clamped edges.

Apart from [6, 7], there are no papers in the open literature on the buckling of thick plates with allowance for *PBD*. Unlike the earlier work on rectangular plates, this present study considers simply supported and clamped circular plates under uniform radial inplane loads.

In determining the buckling load, the Trefftz's initial stress theory [8] is adopted. On the basis of the strain energy functional, the governing differential equations and boundary conditions are derived using calculus of variations. By analytically solving the differential equations, the critical loads may be presented in closed-form expressions. Scalar indicators are embedded in these expressions which enable the inclusion or the exclusion of the influences of *PBD* and the second order terms involving the in-plane deformation in the Green-Lagrangian strain expressions. Note that these second order terms have been referred to in the literature [9, 10] as "curvature terms" (*CT*). Consequently, the sensitivity of the critical load to these individual effects can be examined using these scalar indicators.

2 Derivation of energy functional by Trefftz's theory

Consider an isotropic circular Mindlin plate of uniform thickness t, and radius R under uniform radial compressive in-plane load N as shown in Fig. 1. According to Trefftz's initial stress theory [8], the internal strain energy may be expressed as

$$F = \frac{1}{2}\int_V \varepsilon_L{}^T[B]\,\varepsilon_L\,dV + \int_V \sigma^T\varepsilon_N\,dV \tag{1}$$

in which V is the volume of the plate in the prestressed state; ε is the incremental strain tensor; σ is the prestress tensor; [**B**] is the material property matrix; and the subscripts L and N denote linear and nonlinear components, respectively.

In view of axisymmetric buckling and the assumption of no thickness deformation, the incremental displacements can be expressed in polar coordinates as

$$u_r(r, \phi, z) = -z\theta_r(r), \tag{2a}$$

$$u_\phi(r, \phi, z) = 0, \tag{2b}$$

$$w(r, \phi, z) = w(r), \tag{2c}$$

in which r, ϕ and z are the radial, circumferential and transverse coordinates; u_r, u_ϕ and w are the displacements in the radial, circumferential and transverse directions; and θ_r is the rotation in the radial planes, respectively.

In view of (2), the linear and nonlinear strain tensors are given as follows [11]:

$$\boldsymbol{\varepsilon}_L{}^T = \{\varepsilon_{rrL}\varepsilon_{\phi\phi L}\varepsilon_{zzL}\varepsilon_{r\phi L}\varepsilon_{rzL}\varepsilon_{\phi zL}\}, \tag{3a}$$

in which

$$\varepsilon_{rrL} = \frac{\partial u_r}{\partial r} = -z\frac{d\theta_r}{dr}, \quad \varepsilon_{\phi\phi L} = \frac{1}{r}\frac{\partial u_\phi}{\partial \phi} + \frac{u_r}{r} = -\frac{z}{r}\theta_r, \quad \varepsilon_{zzL} = \frac{\partial w}{\partial z} = 0,$$

$$\varepsilon_{r\phi L} = \frac{1}{r}\frac{\partial u_r}{\partial \phi} + \frac{\partial u_\phi}{\partial r} - \frac{u_\phi}{r} = 0, \quad \varepsilon_{rzL} = \frac{\partial u_r}{\partial z} + \frac{\partial w}{\partial r} = -\left(\theta_r - \frac{dw}{dr}\right), \quad \varepsilon_{\phi zL} = \frac{\partial u_\phi}{\partial z} + \frac{1}{r}\frac{\partial w}{\partial \phi} = 0$$

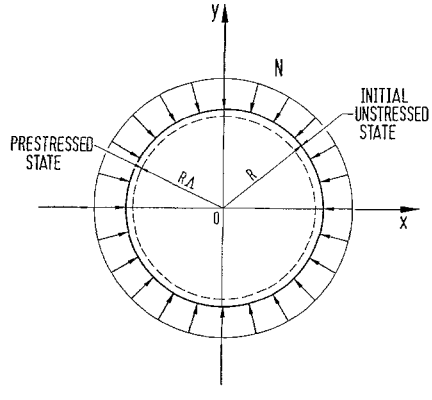

Fig. 1. Buckling of thick circular plate under uniform in-plane load

and

$$\boldsymbol{\varepsilon}_N{}^T = \{\varepsilon_{rrN}\ \varepsilon_{\phi\phi N}\ \varepsilon_{zzN}\ \varepsilon_{r\phi N}\ \varepsilon_{rzN}\ \varepsilon_{\phi zN}\}, \tag{3b}$$

in which

$$\varepsilon_{rrN} = \frac{C_C}{2}\left[\left(\frac{\partial u_r}{\partial r}\right)^2 + \left(\frac{\partial u_\phi}{\partial r}\right)^2\right] + \frac{1}{2}\left(\frac{\partial w}{\partial r}\right)^2 = C_C\frac{z^2}{2}\left(\frac{\mathrm{d}\theta_r}{\mathrm{d}r}\right)^2 + \frac{1}{2}\left(\frac{\mathrm{d}w}{\mathrm{d}r}\right)^2,$$

$$\varepsilon_{\phi\phi N} = \frac{C_C}{2}\left[\left(\frac{1}{r}\frac{\partial u_\phi}{\partial \phi} + \frac{u_r}{r}\right)^2 + \left(\frac{1}{r}\frac{\partial u_r}{\partial \phi} - \frac{u_\phi}{r}\right)^2\right] + \frac{1}{2}\left(\frac{1}{r}\frac{\partial w}{\partial \phi}\right)^2 = C_C\frac{z^2}{2}\left(\frac{\theta_r}{r}\right)^2,$$

$$\varepsilon_{zzN} = \frac{C_C}{2}\left[\left(\frac{\partial u_r}{\partial z}\right)^2 + \left(\frac{\partial u_\phi}{\partial z}\right)^2\right] + \frac{1}{2}\left(\frac{\partial w}{\partial z}\right)^2 = C_C\frac{\theta_r{}^2}{2},$$

$$\varepsilon_{r\phi N} = C_C\left[\left(\frac{\partial u_r}{\partial r}\right)\left(\frac{1}{r}\frac{\partial u_r}{\partial \phi} - \frac{u_\phi}{r}\right) + \left(\frac{\partial u_\phi}{\partial r}\right)\left(\frac{1}{r}\frac{\partial u_\phi}{\partial \phi} + \frac{u_r}{r}\right)\right] + \left(\frac{\partial w}{\partial r}\right)\left(\frac{1}{r}\frac{\partial w}{\partial \phi}\right) = 0,$$

$$\varepsilon_{rzN} = C_C\left[\left(\frac{\partial u_r}{\partial r}\right)\left(\frac{\partial u_r}{\partial z}\right) + \left(\frac{\partial u_\phi}{\partial r}\right)\left(\frac{\partial u_\phi}{\partial z}\right)\right] + \left(\frac{\partial w}{\partial r}\right)\left(\frac{\partial w}{\partial z}\right) = C_C z\theta_r\left(\frac{\mathrm{d}\theta_r}{\mathrm{d}r}\right),$$

$$\varepsilon_{\phi zN} = C_C\left[\left(\frac{\partial u_r}{\partial z}\right)\left(\frac{1}{r}\frac{\partial u_r}{\partial \phi} - \frac{u_\phi}{r}\right) + \left(\frac{\partial u_\phi}{\partial z}\right)\left(\frac{1}{r}\frac{\partial u_\phi}{\partial \phi} + \frac{u_r}{r}\right)\right] + \left(\frac{\partial w}{\partial z}\right)\left(\frac{1}{r}\frac{\partial w}{\partial \phi}\right) = 0,$$

in which the scalar indicator C_C takes on the values of 1 and 0 for including and excluding the CT, respectively.

The material property matrix, [**B**], is given by

$$[\mathbf{B}] = \begin{bmatrix} \frac{E}{1-\nu^2} & \frac{\nu E}{1-\nu^2} & \frac{\nu E}{1-\nu^2} & 0 & 0 & 0 \\ \frac{\nu E}{1-\nu^2} & \frac{E}{1-\nu^2} & \frac{\nu E}{1-\nu^2} & 0 & 0 & 0 \\ \frac{\nu E}{1-\nu^2} & \frac{\nu E}{1-\nu^2} & \frac{E}{1-\nu^2} & 0 & 0 & 0 \\ 0 & 0 & 0 & \frac{E}{2(1+\nu)} & 0 & 0 \\ 0 & 0 & 0 & 0 & \frac{\varkappa E}{2(1+\nu)} & 0 \\ 0 & 0 & 0 & 0 & 0 & \frac{\varkappa E}{2(1+\nu)} \end{bmatrix} \tag{4}$$

in which E, ν and $\varkappa$ are the Young's modulus, Poisson's ratio and shear correction factor, respectively. The values of shear correction factor $\varkappa$ that have been used in the literature are:

$$\varkappa = \frac{5}{6} \quad \text{due to Reissner [1]} \tag{5a}$$

$$\varkappa = \frac{\pi^2}{12} \quad \text{due to Mindlin [2]} \tag{5b}$$

$$\varkappa = \frac{20(1+\nu)}{24+25\nu+\nu^2} \quad \text{due to Nänni [12]} \tag{5c}$$

As these factors do not differ much in value, the Reissner's factor of $\varkappa = 5/6$ is adopted as comparison of solutions will be made with other researchers who have also used this value.

For circular plates under a uniform radial in-plane compressive load, N, the prestress tensor, σ, is given by

$$\boldsymbol{\sigma}^T = \{\sigma_{rrL}\ \sigma_{\phi\phi L}\ \sigma_{zzL}\ \sigma_{r\phi L}\ \sigma_{rzL}\ \sigma_{\phi zL}\} = \left\{-\frac{N}{t}\ \ -\frac{N}{t}\ \ 0\ \ 0\ \ 0\ \ 0\right\} \tag{6}$$

Substituting (3), (4) and (6) into (1) yields

$$F = \frac{1}{2}\int_V \left\{\frac{Ez^2}{1-v^2}\left[\left(\frac{\mathrm{d}\theta_r}{\mathrm{d}r}\right)^2 + \left(\frac{\theta_r}{r}\right)^2 + 2v\left(\frac{\theta_r}{r}\right)\left(\frac{\mathrm{d}\theta_r}{\mathrm{d}r}\right)\right] - \frac{N}{t}\left[\left(\frac{\mathrm{d}w}{\mathrm{d}r}\right)^2\right]\right.$$
$$\left. + \frac{\varkappa E}{2(1+v)}\left[\left(\theta_r - \frac{\mathrm{d}w}{\mathrm{d}r}\right)^2\right] - C_C z^2 \frac{N}{t}\left[\left(\frac{\mathrm{d}\theta_r}{\mathrm{d}r}\right)^2 + \left(\frac{\theta_r}{r}\right)^2\right]\right\} \mathrm{d}V. \tag{7}$$

Note that V is the prestressed volume at the state of incipient buckling and is given by

$$V = \pi(R\Lambda)^2\, t \tag{8}$$

The in-plane deformation factor, Λ, in (8) is defined as

$$\Lambda = 1 - C_P \frac{N}{t}\left(\frac{1-v}{E}\right) = 1 - C_P \frac{k\alpha^2}{12(1+v)} \tag{9}$$

where $\alpha = t/R$ and k is the critical load factor given by

$$k = \frac{NR^2}{D} \tag{10}$$

and $D = Et^3/[12(1-v^2)]$ is the flexural rigidity of the plate. Note that the scalar indicator C_P in (9) takes the values of 1 and 0 for buckling with and without the allowance for *PBD*, respectively.

Normalising coordinate, r, with respect to the deformed radius, $R\Lambda$ and integrating with respect to z, (7) becomes

$$\frac{F}{\pi D} = \int_0^1 \left\{\varrho\left(\frac{\mathrm{d}\theta_r}{\mathrm{d}\varrho}\right)^2 + \frac{1}{\varrho}(\theta_r)^2 + 2v(\theta_r)\left(\frac{\mathrm{d}\theta_r}{\mathrm{d}\varrho}\right) - k\Lambda^2\varrho\left(\frac{\mathrm{d}\bar{w}}{\mathrm{d}\varrho}\right)^2\right.$$
$$\left. + \frac{6\varkappa(1-v)}{\alpha^2}\Lambda^2\varrho\left(\theta_r - \frac{\mathrm{d}\bar{w}}{\mathrm{d}\varrho}\right)^2 - C_C\frac{k\alpha^2}{12}\left[\varrho\left(\frac{\mathrm{d}\theta_r}{\mathrm{d}\varrho}\right)^2 + \frac{1}{\varrho}(\theta_r)^2\right]\right\} \mathrm{d}\varrho \tag{11}$$

in which $\varrho = r/(R\Lambda)$ and $\bar{w} = w/(R\Lambda)$.

3 Governing differential equations and boundary conditions

The minimization of the energy functional given by (11) with respect to $\bar{w}$ and θ_r, using calculus of variations, leads to the following two coupled differential equilibrium equations

$$\left[1 - \frac{k\alpha^2}{6\varkappa(1-v)}\right]\left[\frac{1}{\varrho}\frac{\mathrm{d}\bar{w}}{\mathrm{d}\varrho} + \frac{\mathrm{d}^2\bar{w}}{\mathrm{d}\varrho^2}\right] - \left[\frac{\theta_r}{\varrho} + \frac{\mathrm{d}\theta_r}{\mathrm{d}\varrho}\right] = 0, \tag{12}$$

$$\left[1 - C_C\frac{k\alpha^2}{12}\right]\left[\frac{\theta_r}{\varrho^2} - \frac{1}{\varrho}\frac{\mathrm{d}\theta_r}{\mathrm{d}\varrho} - \frac{\mathrm{d}^2\theta_r}{\mathrm{d}^2\varrho}\right] + \frac{6\varkappa(1-v)\,\Lambda^2}{\alpha^2}\left[\theta_r - \frac{\mathrm{d}\bar{w}}{\mathrm{d}\varrho}\right] = 0. \tag{13}$$

(13) gives $\mathrm{d}\bar{w}/\mathrm{d}\varrho$ as a function of θ_r. Substituting it and its derivatives with respect to ϱ into (12) yields:

$$\frac{\mathrm{d}^3\theta_r}{\mathrm{d}\varrho^3} + \frac{2}{\varrho}\frac{\mathrm{d}^2\theta_r}{\mathrm{d}\varrho^2} + \left(k_0 - \frac{1}{\varrho^2}\right)\frac{\mathrm{d}\theta_r}{\mathrm{d}\varrho} + \frac{1}{\varrho}\left(k_0 + \frac{1}{\varrho^2}\right)\theta_r = 0, \tag{14}$$

where

$$k_0 = \frac{k\Lambda^2}{\Omega\left(1 - \frac{k\alpha^2}{6\varkappa(1-\nu)}\right)} \tag{15}$$

$$\Omega = 1 - C_C \frac{k\alpha^2}{12}. \tag{16}$$

Introducing $\beta = \sqrt{k_0}\,\varrho$ and dividing through (14) by $(k_0)^{3/2}$ leads to

$$\frac{\mathrm{d}^3\theta_r}{\mathrm{d}\beta^3} + \frac{2}{\beta}\frac{\mathrm{d}^2\theta_r}{\mathrm{d}\beta^2} + \left(1 - \frac{1}{\beta^2}\right)\frac{\mathrm{d}\theta_r}{\mathrm{d}\beta} + \frac{1}{\beta}\left(1 + \frac{1}{\beta^2}\right)\theta_r = 0. \tag{17}$$

As for the boundary conditions, they are:

(i) at $\varrho = 0$ (i.e. $\beta = 0$)

$$\theta_r = 0 \tag{18}$$

(ii) at $\varrho = 1$ $\left(\text{i.e. } \beta = \sqrt{k_0}\right)$

$$\theta_r = 0, \quad \text{for clamped plates;} \tag{19a}$$

$$\Omega\frac{\mathrm{d}\theta_r}{\mathrm{d}\beta} + \frac{\nu}{\beta}\theta_r = 0, \quad \text{for simply supported plates.} \tag{19b}$$

Note that (18) is due to axisymmetry while (19b) is furnished by the transversality condition.

4 Analytical solutions

(17) is a first-order Bessel's differential equation and the general solution is

$$\theta_r(\beta) = aJ_1(\beta) + bY_1(\beta) \tag{20}$$

where a and b are constants while $J_1(\circ)$ and $Y_1(\circ)$ are the first-order Bessel functions of the first and second kind, respectively.

In view of (18) and the fact that at $\beta = 0, J_1 = 0$ and $Y_1 = -\infty$, we have $b = 0$. Thus (20) reduces to

$$\theta_r(\beta) = aJ_1(\beta). \tag{21}$$

Substituting (21) into (19) yields the following stability criteria:

(i) for clamped plates:

$$J_1\left(\sqrt{k_0}\right) = 0, \tag{22a}$$

(ii) for simply supported plates:

$$\Omega\sqrt{k_0}\,J_0\left(\sqrt{k_0}\right) - (\Omega - \nu)\,J_1\left(\sqrt{k_0}\right) = 0, \tag{22b}$$

where $J_0(\circ)$ is the zero-order Bessel function of the first kind.

The critical load factor, k, for clamped and simply supported plates, can be obtained by solving respectively (22a) and (22b), in view of (9), (15) and (16).

Analytical solutions, however, can be derived for different combinations of C_P and C_C. Below, we present explicit exact buckling load expressions except for the cases of simply supported plates with $C_C = 1$.

(22a) and (22b) are first solved to yield k_0:

(i) for clamped plates:

$$k_0 \simeq 14.6820, \tag{23a}$$

(ii) for simply supported plates (ignoring *CT*, i.e. $C_C = 0$, $\Omega = 1$):

$$k_0 \simeq 3.3898 + 2.8383\nu - 0.5011\nu^2 + 0.0583\nu^3. \tag{23b}$$

Note that 23b has been obtained from a least square curve fitting exercise.

Substituting (9) and (16) into (15) leads to the cubic equation for the critical load factor k:

$$\{C_P a_P{}^2\}\, k^3 - \{C_P 2a_P + C_C a_C a_S k_0\}\, k^2 + \{1 + [C_C a_C + a_S]\, k_0\}\, k - k_0 = 0, \tag{24a}$$

where:

$$a_C = \frac{\alpha^2}{12}, \tag{24b}$$

$$a_P = \frac{\alpha^2}{12(1+\nu)} = \frac{a_C}{(1+\nu)}, \tag{24c}$$

$$a_S = \frac{\alpha^2}{6\varkappa(1-\nu)} = \frac{2a_C}{\varkappa(1-\nu)}. \tag{24d}$$

Note that by setting the thickness-radius ratio, α, to zero, (24) yields the expected buckling solution for thin plates, i.e. $k = k_0$ (see [13]).

By setting the scalar indicators C_P and C_C to either 1 or 0 the individual and combined effects of *PBD* and *CT*, can be compared and analysed. There are all together four cases:

case (1) $C_C = 0$, $C_P = 0$ (i.e. only *SD* effect):

$$k = \frac{k_0}{1 + a_S k_0} = \frac{k_0}{1 + \dfrac{\alpha^2 k_0}{6\varkappa(1-\nu)}}. \tag{25}$$

This novel simple explicit buckling solution for clamped and simply supported plates resembles the one obtained for the buckling load of Engesser columns under a vertical load (see [13, pp. 133] or [14]). Note that previous buckling studies on thick circular plates [15–17] presented only some numerical solutions while a simple approximate formula was proposed in [18]. It can be seen from (25) that thin plate solution of k_0 is factored down by $1/(1 + a_S k_0)$. This ratio is very nearly equal to unity for very thin plates as $\alpha \to 0$.

case (2) $C_C = 1$, $C_P = 0$ (i.e. *SD* and *CT* effects included):

$$\{a_C a_S k_0\}\, k^2 - \{1 + [a_C + a_S]\, k_0\}\, k + k_0 = 0, \tag{26}$$

$$k = \frac{[1 + (a_C + a_S)\, k_0] - \sqrt{[1 + (a_C + a_S)\, k_0]^2 - 4a_C a_S k_0{}^2}}{2a_C a_S k_0} \tag{27}$$

case (3) $C_C = 0$, $C_P = 1$ (i.e. *SD* and *PBD* effects included):

$$\{a_P{}^2\}\, k^3 - \{2a_P\}\, k^2 + \{1 + a_S k_0\}\, k - k_0 = 0, \tag{28}$$

$$k = \sqrt[3]{P + \sqrt{Q^3 + P^2}} + \sqrt[3]{P - \sqrt{Q^3 + P^2}} - \frac{2}{3a_P}, \tag{29a}$$

where:

$$P = \frac{27a_P k_0 - 18a_S k_0 - 2}{54a_P{}^3} \tag{29b}$$

$$Q = \frac{3a_S k_0 - 1}{9a_P{}^2} \tag{29c}$$

case (4) $C_C = 1$, $C_P = 1$ (i.e. *SD*, *PBD*, and *CT* effects included):

$$\{a_P{}^2\}\, k^3 - \{2a_P + a_C a_S k_0\}\, k^2 + \{1 + [a_C + a_S]\, k_0\}\, k - k_0 = 0, \tag{30}$$

$$k = 2\sqrt{-Q}\cos\left(\frac{\cos^{-1}\left[P/\sqrt{(-Q)^3}\right] + 2\pi}{3}\right) + \frac{2a_P + a_C a_S k_0}{3a_P{}^2}, \tag{31a}$$

where:

$$P = \frac{k_0}{2a_P{}^2} - \frac{(2a_P + a_C a_S k_0)\,(1 + (a_C + a_S)\, k_0)}{6a_P{}^4} + \frac{(2a_P + a_C a_S k_0)^3}{27a_P{}^6}, \tag{31b}$$

$$Q = \frac{1 + (a_C + a_S)\, k_0}{3a_P{}^2} - \frac{(2a_P + a_C a_S k_0)^2}{9a_P{}^4}. \tag{31c}$$

It should be recalled that values of k_0 in (23 b) is not applicable for simply supported plates with $C_C = 1$, and therefore (26), (27), (30) and (31) are valid for clamped plates only.

5 Results and discussions

Before considering the influence of *PBD*, the analytical solutions for *cases (1)* and *(2)*, which neglect the *PBD* effect, are checked with available numerical solutions obtained from previous researchers [15–18]. Table 1 shows the comparison between the results and the close agreement between *case (1)* solutions and that of Kanaka Raju and Rao [15], Dumir [17] and Wang et al. [18] confirms the correctness of the present analytical expressions for the considered case. Note that Chen and Doong [16] results do not appear to have converged to the correct results. It can be observed that when *CT* are taken into consideration (i.e. *case (2)*), the critical loads are lower, especially when t/R is relatively large. This is to be expected since these *CT* increase the specific work of the loadings.

When *PBD* is allowed for, i.e. *cases (3)* and *(4)*, the critical loads become somewhat higher than those of *cases (1)* and *(2)* as shown in Figs. 2 and 3. At $\alpha = 0.2$, the increase in the loads are 6% for clamped plates and 2% for simply supported plates. The larger increase for the clamped plates can be readily explained as the plates undergo greater in-plane deformation prior to buckling due to the higher load values. Comparing the results for *cases (3)* and *(4)*, it can be observed as before, the inclusion of *CT* causes the buckling loads to decrease slightly.

Table 1. Comparison of critical load factor, $k = NR^2/D$, for radially loaded circular plates

Boundary condition	α (t/R)	Other researchers				Present study	
		Kanaka Raju (1983)	Chen (1984)	Dumir (1985)	Wang (1993)	*case (1)*	*case (2)*
Clamped	0.001	14.6825	–	14.6818	14.6819	14.6819	14.6819
	0.01	–	15.9910	–	14.6759	14.6758	14.6741
	0.02	–	15.9641	–	14.6574	14.6574	14.6503
	0.05	14.5299	15.7783	–	14.5296	14.5296	14.4862
	0.10	14.0910	15.1533	–	14.0909	14.0909	13.9338
	0.15	13.4159	–	–	13.4157	14.4158	13.1137
	0.20	12.5725	13.1234	12.5723	12.5725	12.5724	12.1344
Simply supported	0.001	4.1978	–	4.1978	4.1978	4.1978	4.1978
	0.01	–	4.2061	–	4.1973	4.1973	4.1972
	0.02	–	4.2050	–	4.1958	4.1958	4.1953
	0.05	4.1852	4.1929	–	4.1853	4.1853	4.1823
	0.10	4.1481	4.1505	–	4.1480	4.1480	4.1365
	0.15	4.0874	–	–	4.0875	4.0875	4.0627
	0.20	4.0056	3.9897	4.0057	4.0056	4.0056	3.9643

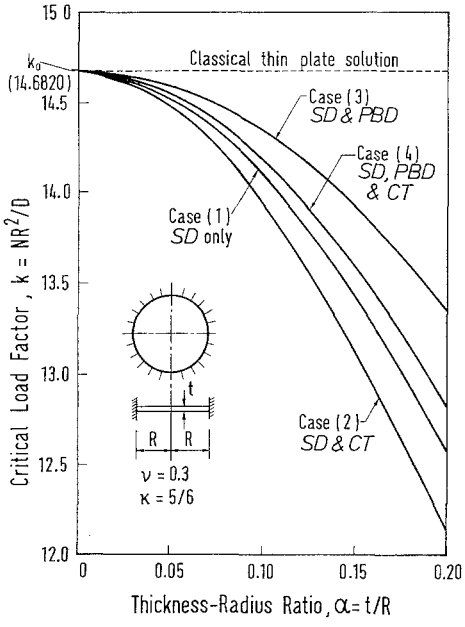

2

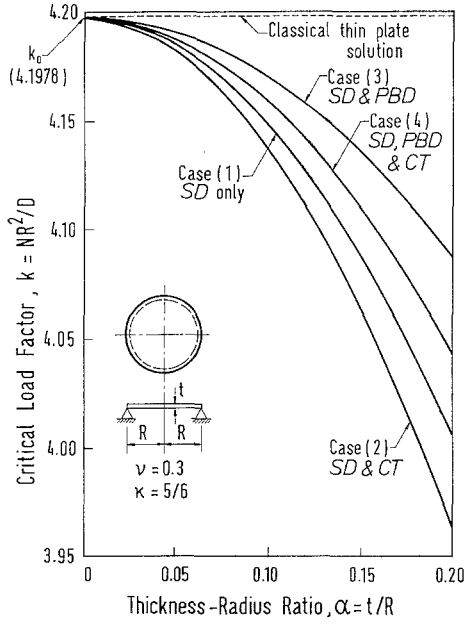

3

Figs. 2 and **3.** **2** Critical load factor k for clamped plates; **3** Critical load factor k for simply supported plates

6 Conclusion

The effect of *PBD* on the elastic critical loads of thick circular plates under uniform radial compression has been investigated. Exact closed-form expressions for the critical load factor k are derived analytically. These analytical expressions should be useful as they provide benchmark values for checking the validity, convergence and accuracy of numerical methods in determining critical loads for thick circular plates.

The effect of *PBD* on the critical load is of the same order of magnitude as the shear effect and both these effects influence the critical loads significantly when the plate thickness is relatively large. While shear deformation causes the critical load to decrease, the pre-buckling inplane deformations cause the critical load to increase. The net result is still a decrement of the critical load and this reduction becomes larger with increasing thickness-radius ratios. Both effects are more pronounced in clamped plates as compared with simply supported ones due to the former plates undergoing greater deformation under larger loads.

The effect of *CT* in the Green-Lagrange strains causes the buckling load to decrease further. This is because the inclusion of the nonlinear terms causes the specific work of the in-plane load to increase, thereby decreasing the critical load. It remains to be verified by future experimental studies on such plate buckling which of the two critical load values, computed with and without *CT*, is more realistic.

Acknowledgement

The project is funded by the research grant RP 910704 made available by the National University of Singapore.

References

1. Reissner, E.: The effect of transverse shear deformation on the bending of elastic plate. J. Appl. Mech. 12 (1945) 69–76
2. Mindlin, R. D.: Influence of rotary inertia and shear in flexural motion of isotropic elastic plates. J. Appl. Mech. 18 (1951) 1031–1036
3. Kollbrunner, C. F.; Herrmann, G.: Einfluß des Schubes auf die Stabilität der Platten im elastischen Bereich. Mittlgn. der T.K.V.S.B., H. 14. Zürich: Verlag V.S.B. 1956

4. Herrmann, G.; Armenakas, A. E.: Vibrations and stability of plates under initial stress. Proc. ASCE / J. Eng. Mech. Div. 86 (1960) 65–94
5. Srinivas, S.; Rao, A. K.: Bending, vibration and buckling of simply supported orthotropic rectangular plates and laminates. Int. J. Solids and Struct. 6 (1970) 1463–1481
6. Ziegler, H.: The influence of inplane deformation on the buckling loads of isotropic elastic plates. Ing. Arch. 53 (1983) 61–72
7. Xiang, Y.; Wang, C. M.; Liew, K. M.; Kitipornchai, S.: Mindlin plate buckling with pre-buckling in-plane deformation. J. Engng. Mech. 119 (1) (1993) 1 – 18
8. Trefftz, E.: Zur Theorie der Stabilität des elastischen Gleichgewichts. ZAMM 12 (1933) 160–165
9. Brunelle, E. J.; Robertson, S. R.: Initially stressed Mindlin plates. AIAA J. 12 (1974) 1036–1045
10. Roufaeil, O. L.; Dawe, D. J.: Rayleigh-Ritz vibration analysis of rectangular Mindlin plates subjected to membrane stresses. Journal of Sound and Vibration 85 (1982) 263–275
11. Saada, A. S.: Elasticity theory and applications. New York: Pergamon Press 1974
12. Nänni, J.: Das Eulersche Knickproblem unter Berücksichtigung der Querkräfte. ZAMP 22 (1971) 156–186
13. Timoshenko, S. P.; Gere, J. M.: Theory of elastic stability. New York: McGraw-Hill 1961
14. Ziegler, H.: Arguments for and against Engesser's buckling formulas. Ing. Arch. 52 (1982) 105–113
15. Kanaka Raju, K.; Venkateswara Rao, G.: Post-buckling analysis of moderately thick elastic circular plates. Trans. ASME / J. Appl. Mech. 50 (1983) 468–470
16. Chen, L. W.; Doong, J. L.: Post-buckling behavior of a thick circular plate. AIAA J. 22 (1984) 564–566
17. Dumir, P. C.: Axisymmetric postbuckling of orthotropic tapered thick annular plates. Trans. ASME / J. Appl. Mech. 52 (1985) 725–727
18. Wang, C. M.; Xiang, Y.; Kitipornchai, S.; Liew, K. M.: Axisymmetric buckling of circular Mindlin plates with ring supports. J. Engng. Mech. 119 (3) (1993) 782 – 793

Received December 22, 1992

Dr. G. M. Hong, Lecturer
Dr. C. M. Wang, Senior Lecturer
Mr. T. J. Tan, Research Assistant
Department of Civil Engineering
National University of Singapore
Kent Ridge, Singapore 0511
Singapore